2014-01-1986
Published 04/01/2014

doi:10.4271/2014-01-1986
saematman.saejournals.org

Failure Mode and Fatigue Behavior of Dissimilar Laser Welds in Lap-Shear Specimens of Aluminum and Copper Sheets

Wei-Jen Lai, Shin-Jang Sung, and Jwo Pan
Univ. of Michigan

Yunan Guo and Xuming Su
Ford Motor Co.

ABSTRACT

Failure mode and fatigue behavior of dissimilar laser welds in lap-shear specimens of aluminum and copper sheets are investigated. Quasi-static tests and fatigue tests of laser-welded lap-shear specimens under different load ranges with the load ratio of 0.1 were conducted. Optical micrographs of the welds after the tests were examined to understand the failure modes of the specimens. For the specimens tested under quasi-static loading conditions, the micrograph indicates that the specimen failed through the fusion zone of the aluminum sheet. For the specimens tested under cyclic loading conditions, two types of failure modes were observed under different load ranges. One failure mode has a kinked crack initiating from the interfacial surface between the aluminum and copper sheets and growing into the aluminum fusion zone at an angle close to 90°. The other failure mode has an interfacial crack initiating at the interfacial surface between the aluminum and copper sheets and growing along the interfacial surface between the fusion zone and the copper base metal at an angle close to 90°. In general, the fatigue lives are longer for the specimens failed through the copper sheet than those failed through the aluminum fusion zone.

CITATION: Lai, W., Sung, S., Pan, J., Guo, Y. et al., "Failure Mode and Fatigue Behavior of Dissimilar Laser Welds in Lap-Shear Specimens of Aluminum and Copper Sheets," *SAE Int. J. Mater. Manf.* 7(3):2014, doi:10.4271/2014-01-1986.

INTRODUCTION

With the growing demand of highly compact, complex and integrated designs, joining dissimilar materials has become an important and inevitable trend in product manufacturing. Welding techniques such as laser welding, ultrasonic welding, and friction stir welding demonstrate different capabilities and advantages in joining dissimilar materials. In the hybrid and electric vehicles, joining the aluminum and copper tabs in battery packs is especially critical since the weld quality is closely related to the battery safety. Recently, research works have been focused on welding aluminum and copper using laser welding technique [1, 2, 3, 4]. Laser welding has many advantages over other welding techniques such as precise spatial and temporal controls in heat input, high flexibility and repeatability, and relatively small heat affected zone [5,6].

Joining aluminum and copper has several potential difficulties. Metallurgically, aluminum and copper forms various hard and brittle intermetallic phases such as Al_4Cu_9, Al_3Cu_4, AlCu, and Al_2Cu according to the phase diagram. These intermetallic phases tend to form in the fusion zone, and deteriorate the mechanical properties of the weld. In order to overcome this problem, some filler materials such as silver, nickel, and lead were reported to successfully minimize the formation of the intermetallic phases [4]. Decreasing the heat input using a small spot diameter and increasing cooling rate using short pulse width laser also help suppress the formation of the intermetallic phases. Other issues such as large differences in thermal expansion and heat capacity also pose significant challenges to laser weld the two materials.

In this paper, the failure mode and fatigue behavior of dissimilar laser welds in lap-shear specimens of aluminum and copper sheets are examined. Laser welded lap-shear specimens were first made from dissimilar aluminum and copper sheets. These lap-shear specimens were then machined into a dog-bone shape to remove the notches on the edges of the welds. Next, the lap-shear specimens were tested under quasi-static and cyclic loading conditions. Quasi-static and fatigue strengths of the welds in the lap-shear specimens were then obtained and examined. Optical micrographs of failed specimens after testing were also examined to identify the failure modes of the specimens. Finally, conclusions are made based on the experimental results.

EXPERIMENT

Aluminum and copper sheets with the thicknesses of 0.8 mm and 1.6 mm, respectively, are used in this investigation. Laser welded lap-shear specimens were prepared for this study. Each lap-shear specimen was made by using a 25 mm × 95 mm aluminum and a 25 mm × 95 mm copper sheet with a 13 mm × 25 mm overlap area. The chemical compositions and mechanical properties of the aluminum and copper sheets provided by the manufacturers are listed in Table 1 and 2, respectively.

Table 1. Chemical compositions of the aluminum and copper sheets.

	Si	Fe	Cu	Zn	Others	Al
Al-1100 H18	0.05	0.6	0.11	0.01	0.15	99.00
Cu-C1100 H00	-	-	99.97 (includes Ag)	-	-	-

Table 2. Mechanical properties of the aluminum and copper sheets.

	Yield strength (MPa)	Tensile strength (MPa)	Elongation (%)
Al-1100 H18	166	170	6
Cu-C1100 H00	-	276	20

Figure 1(a) shows a top view of a laser-welded lap-shear specimen before machining and Figures 1(b) shows the corresponding schematic of the top and side views with doublers. The loading direction is shown by the arrows. The two laser welds are shown as the gray lines in Figures 1(b).

For the lap-shear specimens, the aluminum and copper sheets were welded using fiber laser with a laser power of 3.0 kW and a welding speed of 7.0 m/min. Argon was used during the welding process as the shielding gas with a discharge rate of 40 CFM. The laser beam was incident on the aluminum sheet and welded the two sheets together. Two welds were made in two passes from one side to the other. The right weld was made by the first pass and the left weld was made by the second pass, as shown in Figure 1(a). No heat treatment was carried out after the welding process. Figure 1(a) shows the welds on the upper aluminum sheet of the lap-shear specimen with a weld width of 2 mm.

(a)

Figure 1.

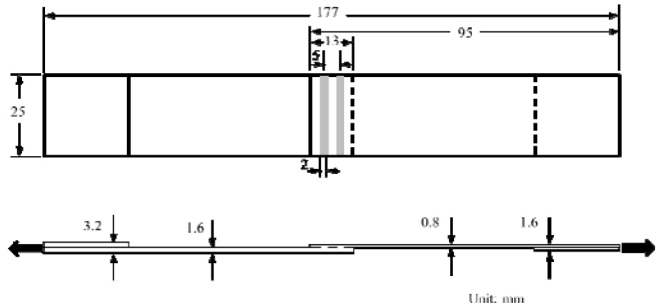

(b)

Figure 1. (cont.) (a) A top view of a laser-welded lap-shear specimen before machining and (b) the corresponding schematics of the top and side views with the loading direction shown by the arrows. The gray lines represent the welds.

After the lap-shear specimens were made, the specimens were then machined into a dog-bone shape to remove the notches on the edges of the welds, as marked in Figure 2. Preliminary test results have shown that the notches affected the test results. Therefore, the stress concentrations due to the notches need to be removed. Figure 3(a) shows a top view of a laser-welded lap-shear specimen after machining and Figures 3(b) shows the corresponding schematic of the top and side views with doublers. In the figures, the loading direction is shown by the arrows. The two laser welds are shown as the gray lines in Figures 3(b).

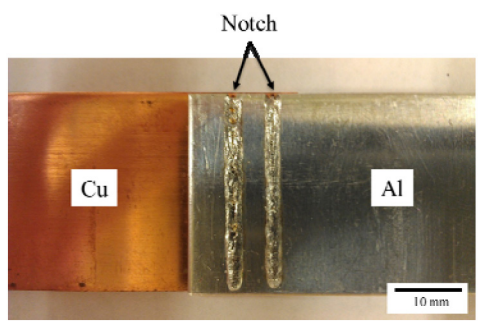

Figure 2. A closed-up view of a laser-welded lap-shear specimen showing the notches on the edges of the welds.

(a)

Figure 3. (a) A top view of a laser-welded lap-shear specimen after machining and (b) the corresponding schematics of the top and side views with the loading direction shown by the arrows. The gray lines represent the welds.

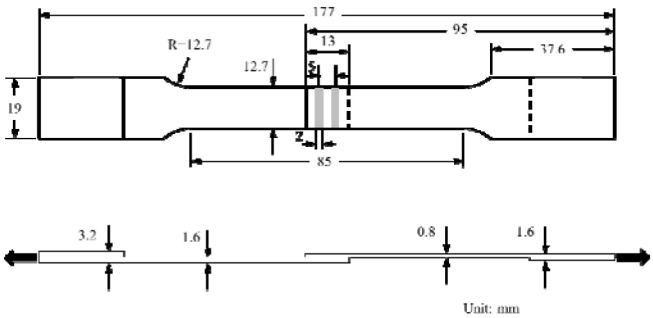

(b)

Figure 3. (cont.) (a) A top view of a laser-welded lap-shear specimen after machining and (b) the corresponding schematics of the top and side views with the loading direction shown by the arrows. The gray lines represent the welds.

Prior to testing, one lap-shear specimen was sectioned through the center line parallel to the loading direction to observe the cross section of the welded region. The lap-shear specimens were first tested with doublers under quasi-static loading conditions by using a MTS testing machine at a displacement rate of 5 mm/min. Only two specimens were tested under quasi-static loading conditions due to the limited number of available specimens. The average failure load, defined as the average of the maximum loads of the load-displacement curves obtained from the two lap-shear specimens, is 769 N. The failure loads of the two specimens are 798 N and 739 N, respectively. The average failure load was used as the reference load to determine the applied loads for the fatigue tests. The lap-shear specimens were then tested with doublers under cyclic loading conditions using an Instron servo-hydraulic fatigue testing machine with the load ratio of 0.1. The test frequency was 10 Hz. The tests were terminated when specimens were separated or transverse cracks from the welds became clearly visible. Figure 4 shows the load ranges as functions of the fatigue life for the lap-shear specimens under cyclic loading conditions. As marked in Figure 4, specimens can fail in either the aluminum or copper sheets.

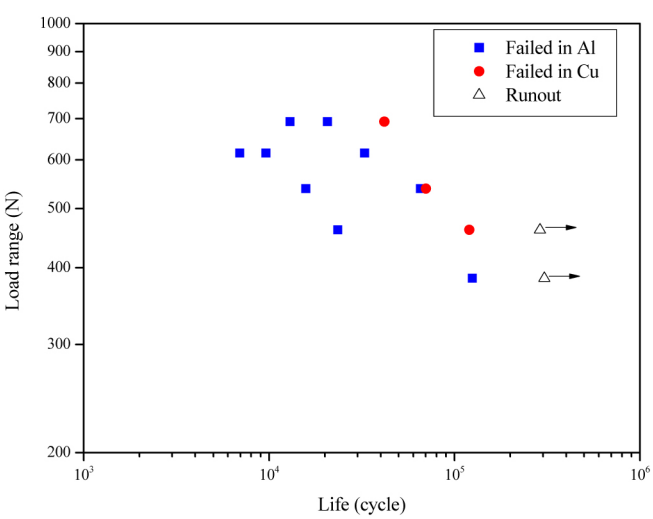

Figure 4. Experimental results of the fatigue tests for the laser-welded lap-shear specimens under the load ratio of 0.1.

FAILURE MODE

Figure 5(a) shows the symmetry cross section of an untested specimen. The fusion zone can be clearly seen in the figure. Many voids were observed in or near the fusion zone, and the size and location of these voids may vary, as indicated by red arrows. The fusion zone is wider in the aluminum sheet and is smaller in the copper sheet due to the lower thermal diffusivity and lower melting temperature of the aluminum as well as the lower viscosity of the molten aluminum. The microstructure of the fusion zone in the copper sheet also shows material flow occurring during the welding process. It is noted that the actual joined width of the weld is about 1 mm.

Figure 5(b) shows the symmetry cross section of a failed specimen under quasi-static loading conditions. The micrograph indicates that the specimen failed through the fusion zone of the aluminum sheet. It should be noted that an interfacial crack was formed along the interfacial surface between the fusion zone and the copper base metal. Figure 5(c) shows a schematic of the failure mode of the aluminum sheet of the specimen under quasi-static loading conditions.

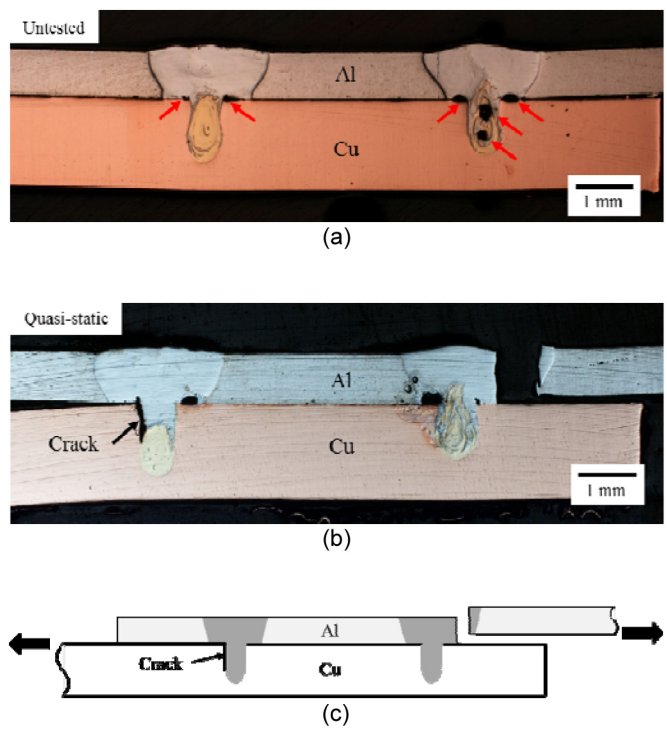

Figure 5. Optical micrographs of the cross sections along the symmetry planes of (a) an untested specimen and (b) a failed specimen under quasi-static loading conditions. The red arrows indicate the voids. (c) A schematic of the failure mode under quasi-static loading conditions.

Under cyclic loading conditions, two types of failure modes were observed, as marked in Figure 4. Figure 6(a) shows the symmetry cross section of a failed specimen caused by the kinked crack failure mode in the aluminum fusion zone at the fatigue life of 2.3×10^4 cycles under a load range of 416 N. As shown in the figure, the kinked crack was initiated from the interfacial surface between the aluminum and copper sheets and grew into the aluminum fusion zone at an angle close to

90°. As schematically shown, an interfacial crack grew along the interfacial surface between the fusion zone and the copper base metal but did not grow through the copper sheet. Figure 6(b) shows the symmetry cross section of a failed specimen caused by the interfacial crack failure mode between the fusion zone and the copper base metal at the fatigue life of 1.2×10^5 cycles under a load range of 416 N. As shown in the figure, the interfacial crack grew along the interfacial surface between the fusion zone and the copper base metal, and the crack finally grew through the copper sheet. Note that no kinked crack was observed in and near the aluminum fusion zone. Figures 6(c) and 6(d) show schematics of the kinked crack and interfacial crack failure modes occurring in the aluminum fusion zone and between the fusion zone and the copper base metal under cyclic loading conditions, respectively.

As shown in Figure 4, the two failure modes under cyclic loading conditions were observed under different load ranges. In general, the fatigue lives are longer for the specimens failed through the copper sheet than those failed in the aluminum fusion zone. This might be due to the fact that the copper sheet is thicker or the copper used in this study might have better fatigue strengths than those of the aluminum base metal and the fusion zone. The reason that one failure mode prevails over the other under cyclic loading conditions is unclear. One possible reason is the highly unpredictable nature of the size and location of the void defects due to the welding process. The void defects near the fusion zone between the two sheets can cause different degrees of stress concentration due to the notch effect. If the notch effect is significant for the kinked crack to initiate in the aluminum fusion zone, the specimen might have a higher chance to fail through the aluminum fusion zone. On the other hand, if the void defect is not significant, the interfacial crack between the fusion zone and the copper sheet might have a higher chance to lead to the final failure.

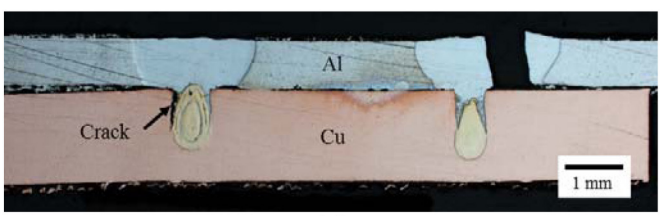

(a)

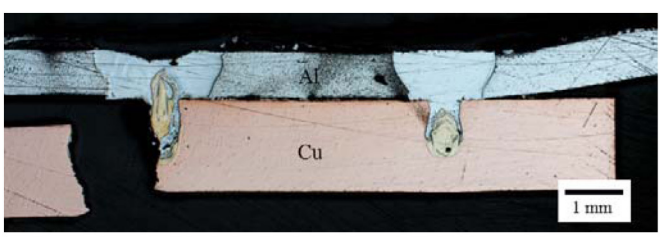

(b)

Figure 6.

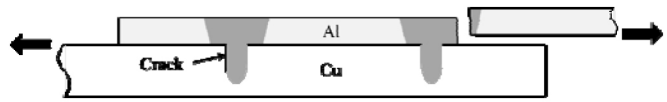

(c)

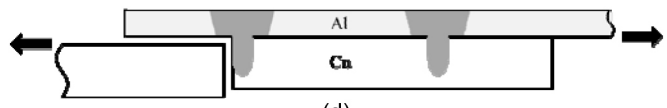

(d)

Figure 6. (cont.) Optical micrographs of the cross sections along the symmetry planes of (a) a failed specimen at the fatigue life of 2.3×10^4 cycles under a load range of 416 N and (b) a failed specimen at the fatigue life of 1.2×10^5 cycles under a load range of 416 N. Schematics of the failure modes occurring through (a) the aluminum fusion zone and (b) the copper sheet under cyclic loading conditions.

The crack formation along the interfacial surface of the fusion zone and the copper base metal was observed in the specimens failed under both quasi-static and cyclic loading conditions. This suggests that the interfacial surface is relatively weak in strength compared to those of the nearby fusion zone and the copper base metal.

SUMMARY/CONCLUSIONS

Failure mode and fatigue behavior of dissimilar laser welds in lap-shear specimens of aluminum and copper sheets are investigated. Quasi-static tests and fatigue tests of laser-welded lap-shear specimens under different load ranges with the load ratio of 0.1 were conducted. Optical micrographs of the welds after the tests were examined to understand the failure modes of the specimens. For the specimens tested under quasi-static loading conditions, the micrograph indicates that the specimen failed through the fusion zone of the aluminum sheet. For the specimens tested under cyclic loading conditions, two types of failure modes were observed under different load ranges. One failure mode has a kinked crack initiating from the interfacial surface between the aluminum and copper sheets and growing into the aluminum fusion zone at an angle close to 90°. The other failure mode has an interfacial crack initiating at the interfacial surface between the aluminum and copper sheets and growing along the interfacial surface between the fusion zone and the copper base metal at an angle close to 90°. In general, the fatigue lives are longer for the specimens failed through the copper sheet than those failed through the aluminum fusion zone. The highly unpredictable nature of the size and location of the void defects due to the welding process could determine the final failure mode for the specimens tested under cyclic loading conditions.

REFERENCES

1. Balu, P., Carlson, B., Kovacevic, R., "An Investigation into the Laser Micro-Welding of Aluminum and Copper in Lap Joint Configuration," TMS annual Meeting 3:295-307, 2011, doi:10.1002/9781118062173.ch37.
2. Mai, T., Spowage, A., "Characterization of Dissimilar Joints in Laser Welding of Steel-Kovar, Copper-Steel and Copper-Aluminum," Materials Science and Engineering A 374:224-233, 2004, doi:10.1016/j.msea.2004.02.025.

3. Solchenbach, T., Plapper, P., "Mechanical Characteristics of Laser Braze-Welded Aluminum-Copper Connections," Optics & Laser Technology 54:249-256, 2013, doi:10.1016/j.optlastec.2013.06.003.
4. Weigl, M., Albert, F., Schmidt, M., "Enhancing the Ductility of Laser-Welded Copper-Aluminum Connections by Using Adapted Filler Materials," Physics Procedia 12:332-338, 2011, doi:10.1016/j.phpro.2011.03.141.
5. Kannatey-Asibu, E., "Principles of Laser Material Processing," Wiley, 2009.
6. Steen, W., Mazumder, J., "Laser Material Processing," 4th edition, Springer, 2010, doi:10.1007/978-1-84996-062-5.

CONTACT INFORMATION

Professor Jwo Pan
Mechanical Engineering
The University of Michigan
Ann Arbor, MI 48109-2125
Telephone: 734-764-9404
Fax: 734-647-3170
jwo@umich.edu